Acta Crystallographica Section B
Structural Science
ISSN 0108-7681

Conformational analysis: crystallographic, molecular mechanics and quantum chemical studies of C—H···O hydrogen bonding in the flexible bis(nosylate) derivative of catechol

Orde Quentin Munro* and Lynette Mariah

University of KwaZulu-Natal, Private Bag X01, Scottsville 3209, Pietermaritzburg, South Africa

Correspondence e-mail: munroo@ukzn.ac.za

Received 26 March 2004
Accepted 10 August 2004

The single-crystal X-ray diffraction analysis of 2-{[(4-nitrophenoxy)sulfonyl]oxy}phenyl 4-nitrophenyl sulfate (4) reveals that an interesting intermolecular or extended structure (a one-dimensional hydrogen-bonded polymer) is formed because of pairs of intermolecular (aryl)C—H···O(nitro) hydrogen bonds between the C_2 symmetry monomer units. The axis of the hydrogen-bonded polymer runs co-linear with the [101] face diagonal of the monoclinic unit cell. Molecular mechanics calculations using a modified version of the *MM*+ force field and a random conformational search algorithm have been used to locate the important low-energy *in vacuo* conformations of (4). The *MM*-calculated conformation of (4) that most closely matches the X-ray structure lies some 26.5 kJ mol^{-1} higher in energy than the global minimum-energy conformation, consistent with the notion that the crystallographically observed molecular architecture of (4) is a local energy minimum in the absence of its crystal lattice environment. Since the X-ray conformation of (4) was correctly calculated only when all of the neighbouring molecules in the crystal lattice were included in the simulation, hydrogen bonding and other non-bonded interactions in the crystal lattice clearly dictate the experimentally observed conformation of (4). Quantum chemical calculations (*AM*1 method) confirm the critical role played by the intermolecular (aryl)C—H···O(nitro) hydrogen bonds in controlling the crystallographically observed conformation of (4) and show that self-recognition in this system by hydrogen bonding is favoured on electrostatic grounds. Collectively, the molecular simulations suggest that because the lowest-energy *molecular* conformation of (4) does not permit the formation of an extended hydrogen-bonded 'supramolecular' structure, it is not the preferred conformation in the crystalline solid state.

1. Introduction

The reaction of an alcohol with 4-nitrobenzenesulfonyl chloride (1) (commonly known as nosyl chloride) affords the corresponding alkyl/aryl 4-nitrobenzenesulfonate or nosylate derivative (2). This type of product is particularly useful as a synthetic intermediate and its formation is commonly used as a convenient method of activating primary or secondary alcohols prior to their substitution with a nucleophile (March, 1985). In effect, nosylates are good leaving groups provided that the *R* group is aliphatic and not unduly sterically hindered. In the case of aromatic alcohols, benzenesulfonyl chloride derivatives may be employed as stable blocking groups since substitution is not possible by a normal S_N2 mechanism under standard conditions (Carey & Sundberg, 1990).

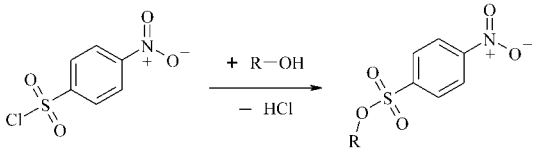

(1) (2)

We have recently developed a new molecular mechanics (*MM*) force field for modelling the structures of aromatic sulfonic esters (including nosylates) and have shown (by X-ray crystallography and *MM* simulations) that the aryl groups of these simple compounds behave as good aromatic acceptor units that are capable of associating by intra- or intermolecular $\pi\cdots\pi$ interactions with other aromatic groups (Munro *et al.*, 2003). In the case of the nosylate derivative, 2-(6-iodo-1,3-benzodioxol-5-yl)ethyl 4-nitrobenzenesulfonate (3), this was found to favour a hairpin-shaped conformation in which the 4-nitrobenzene group stacked in a near-parallel intramolecular fashion with the 1,3-benzodioxole ring. However, we also found that one of the nitro-group O atoms formed a soft intermolecular hydrogen bond of 2.5 Å with the H atom of a neighbouring molecule's aromatic C—H group. Interestingly, because the π-stacking or ring$\cdots$ring interaction in this system was dominant, the conformation of (3) in the solid state did not differ significantly from the calculated gas-phase conformation, *i.e.* the intermolecular (aryl)C—H$\cdots$O(nitro) hydrogen-bonding interactions in the crystal structure of (3) had no major impact on the crystallographically observed conformation.

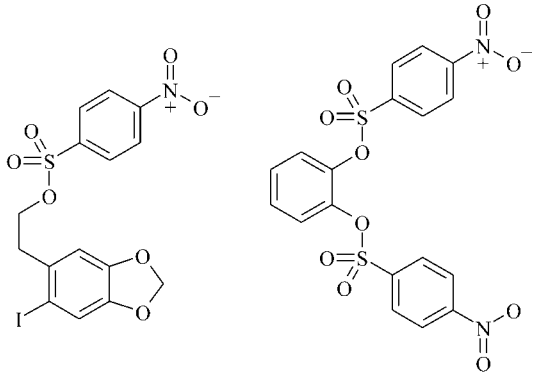

(3) (4)

In this paper we report the synthesis and characterization of the novel bis(nosylate) derivative of catechol (4), which has the correct functional groups for only two important types of intermolecular interaction, namely hydrogen bonding [both (aryl)C—H$\cdots$O(nitro) and (aryl)C—H$\cdots$O(sulfonyl)] and aromatic $\pi\cdots\pi$ stacking, in addition to possible intramolecular $\pi\cdots\pi$ interactions. Our goal was to crystallize a compound with limited options as far as these interactions are concerned in an effort to shed further light on their relative importance not only for nosylates, but in fact for any compound with similar functional groups. Indeed, as shown recently by Ferguson's group (Bowes *et al.*, 2003) and others (Braga *et al.*, 1995; Mowbray *et al.*, 1999), C—H$\cdots$O hydrogen bonding is often responsible for the finer aspects of an extended solid-state or 'supramolecular' structure in systems where such interactions occur (Langley *et al.*, 1998) and accordingly cannot be overlooked. Indeed, the fundamental importance of weak C—H$\cdots$O hydrogen bonding in chemical and biological systems has inspired a recent book on the subject (Desiraju & Steiner, 1999). Moreover, although X-ray structural and computational investigations of hydrogen-bonding systems date back several decades (Leiserowitz, 1976; Del Bene & Kochenour, 1976), considerable effort is currently focused (Coupar *et al.*, 1997; Ferguson *et al.*, 1997; Sørensen & Larsen, 2003) on understanding crystal-packing interactions (particularly hydrogen bonds) at a level that may one day underpin the development of calculation methods that accurately predict crystal structures for small molecules. Lastly, the formation of hydrogen bonds in several types of nitro compound has attracted considerable theoretical and experimental interest (Szczesna & Urbanczyk-Lipkowska, 2002; Chen & Tzeng, 1999; Hanuza *et al.*, 1998) due mainly to the ubiquity of organic nitro derivatives, their use as explosives (Bemm & Ostmark, 1998) and the generally strong hydrogen-bond acceptor character of nitro group O atoms (Wolff *et al.*, 1999; Yan & Zhu, 1999; Rablen *et al.*, 1998).

Our strategy herein has been to use a combination of low-temperature X-ray crystallography, semi-empirical quantum chemical calculations (*AM*1 method; Dewar *et al.*, 1985) and *MM* simulations to study both the intermolecular interactions and low-energy conformations of (4). Fascinatingly, (4) exhibits an extended intermolecular structure that is best described as an elegant (aryl)C—H$\cdots$O(nitro) hydrogen-bonded polymer with favourable hydrogen-bond donor/acceptor complementarity that is characterized by the seven-membered ring structure illustrated below.

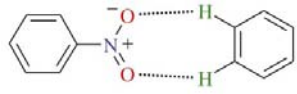

To our knowledge, (4) appears to be the only crystallographically characterized *nosylate derivative* for which a near-symmetrical hydrogen-bonding interaction involving both nitro O atoms and a pair of aromatic or aliphatic C—H group H atoms has been observed. Furthermore, and in contrast to (3), aromatic $\pi\cdots\pi$ interactions appear to play a negligible role in determining the extended solid-state structure in this system, even though they are theoretically possible. Interestingly, four other (aryl)C—H$\cdots$O(nitro) hydrogen-bonding modes have recently been identified (in addition to aromatic $\pi\cdots\pi$ interactions) in solvates of the supramolecular host compound tetrakis(4-nitrophenyl)methane (Thaimattam *et al.*, 2001), suggesting that such interactions are probably more ubiquitous and significant than might be anticipated at first glance.

Table 1
Crystal data and structure refinement details for (4).

Crystal data	
Chemical formula	$C_{18}H_{12}N_2O_{10}S_2$
M_r	480.42
Cell setting, space group	Monoclinic, *C*2/*c*
a, *b*, *c* (Å)	11.667 (11), 10.803 (11), 15.868 (16)
β (°)	108.20 (9)
V (Å^3)	1900 (3)
Z	4
D_x (Mg m^{-3})	1.680
Radiation type	Mo $K\alpha$
No. of reflections for cell parameters	105
θ range (°)	4–32
μ (mm^{-1})	0.35
Temperature (K)	100 (2)
Crystal form, colour	Plate, colourless
Crystal size (mm)	0.50 × 0.40 × 0.10
Data collection	
Diffractometer	Oxford Diffraction Xcalibur 2CCD
Data collection method	ω–2θ scans
Absorption correction	Multi-scan (based on symmetry-related measurements)
T_{min}	0.846
T_{max}	0.966
No. of measured, independent and observed reflections	38 881, 3744, 3259
Criterion for observed reflections	$I > 2\sigma(I)$
R_{int}	0.038
θ_{max} (°)	34.1
Range of *h*, *k*, *l*	$-18 \Rightarrow h \Rightarrow 18$ $-16 \Rightarrow k \Rightarrow 16$ $-24 \Rightarrow l \Rightarrow 24$
Refinement	
Refinement on	F^2
$R[F^2 > 2\sigma(F^2)]$, $wR(F^2)$, *S*	0.046, 0.116, 1.14
No. of reflections	3744
No. of parameters	169
H-atom treatment	Refined independently
Weighting scheme	$w = 1/[\sigma^2(F_o^2) + (0.049P)^2 + 2.7297P]$, where $P = (F_o^2 + 2F_c^2)/3$
$(\Delta/\sigma)_{max}$	<0.0001
$\Delta\rho_{max}$, $\Delta\rho_{min}$ (e Å^{-3})	0.52, −0.45

Computer programs used: *CrysAlis CCD* 170 (Oxford Diffraction, 2002), *SHELXS*97 (Sheldrick, 1997), *SHELXL*97 (Sheldrick, 1997), *WinGX* (Farrugia, 1999).

Lastly, our calculations clearly show that the gas-phase conformation of (4) that most closely matches the X-ray crystal structure is a *local energy minimum* with C_2 symmetry. The conformation of (4) observed in the solid state therefore differs significantly from the calculated lowest-energy C_1 symmetry conformation in the gas phase, a finding which demonstrates that when conformational energy differences are small, the quest for a more favourable lattice energy (in this case crystallization in the space group *C*2/*c* on a twofold axis with the concomitant formation of extended intermolecular interactions) apparently overrides the quest for a lower *conformational* energy. The stability of the crystal lattice of (4) apparently results mainly from the network of intermolecular (aryl)C—H···O(nitro) interactions, consistent with the conclusion reached by others for a system having ostensibly similar weak hydrogen bonds (Thaimattam *et al.*, 2001).

2. Experimental

2.1. General information

All manipulations were carried out under nitrogen using oven-dried glassware. Tetrahydrofuran (THF) and hexane were freshly distilled over sodium/benzophenone. Catechol (benzene-1,2-diol) and 4-nitrobenzenesulfonyl chloride (1) were used as received (Aldrich). Triethylamine (BDH) was distilled over CaH_2 immediately before use. Electronic spectra were recorded with a Perkin–Elmer Lambda 45 double-beam spectrophotometer using THF solutions in 1.0 cm path-length cuvettes. Samples for IR spectroscopy were KBr mulls of polycrystalline material. FT-IR spectra were recorded with a Perkin–Elmer Spectrum One spectrometer (4 scans, spectral resolution = 1.0 cm^{-1}). Microanalytical data were obtained from a polycrystalline sample of (4) using a LECO CHNS-932 instrument. NMR spectra were recorded in acetone-d_6 with a 500 MHz Varian Unity Inova spectrometer equipped with an Oxford magnet (11.744 T). Standard pulse sequences were employed.

2.2. Synthesis of (4)

A solution of catechol (2.42 g, 22.0 mmol) dissolved in 100 ml of THF was added to a solution of (1) (11.08 g, 50.0 mmol) dissolved in 100 ml of THF, to which triethylamine (5 ml, 70 mmol) had been added. The reaction was allowed to proceed with stirring for 48 h at room temperature under nitrogen. Precipitated Et_3NHCl (white solid) was removed by filtration prior to the removal of the solvent by rotary evaporation. The orange solid was redissolved in chloroform (20 ml). The addition of water (20 ml) facilitated the precipitation of (4) as a beige powder, which was collected by filtration and washed with diethyl ether. The product (cream-coloured powder) was air-dried. Yield: 7.98 g, 83%. Anal.: calcd for $C_{18}H_{12}N_2O_{10}S_2$: C 45.0, H 2.52, N 5.83, O 33.3, S 13.4; found: C 44.4, H 2.12, N 5.98, S 13.18. UV–vis (THF) [λ_{max}, nm]: 250, 290 (shoulder). δ_H (p.p.m., 500 MHz, acetone-d_6) 8.17 (2H, dd, ^3J = 6.1 Hz, ^4J = 3.7 Hz, C*H*), 8.29 (2H, dd, ^3J = 6.3 Hz, ^4J = 3.7 Hz, C*H*CO), 8.92 (4H, d, ^3J = 8.9 Hz, C*H*CS), 9.30 (4H, d, ^3J = 9.0 Hz, C*H*CNO$_2$). δ_C (p.p.m., 125 MHz, acetone-d_6) 125.73 (*C*HCHCO), 125.81 (*C*HCN), 131.09 (*C*HCS), 130.12 (*C*HCO), 141.31 (*C*S), 141.82 (*C*O), 152.61 (*C*N). IR (KBr pellet, cm^{-1}) 3110 [w, ν(CH)], 3070 [w, ν(CH)], 1610 (w), 1532 [s, ν_a(NO$_2$)], 1485 (w), 1389 [m, ν_a S(=O)$_2$], 1359 [s, ν_s(NO$_2$)], 1228 (w), 1200 [s, ν_s S(=O)$_2$], 1081 (m), 889 (m), 836 (m), 748 (m), 646 (w).

2.3. X-ray crystallography

X-ray diffraction data from a colourless plate-shaped crystal of (4) (obtained from THF/hexane) with the approximate dimensions 0.1 × 0.4 × 0.5 mm^3 were collected with *CrysAlis CCD 170* (Oxford Diffraction, 2002) on an Oxford Diffraction Xcalibur 2CCD four-circle diffractometer fitted with an Oxford Instruments Cryojet operating at 100 (2) K. The data were collected at a crystal-to-detector distance of 50 mm using ω scans at θ = 34.364° with 12 s exposures taken at 2.10 kW X-

ray power with 1.0° frame widths. A complete data sphere was collected in 12 sequential ω scans using different κ orientations and φ ranges. The data were reduced with the program *CrysAlis RED 170* (Oxford Diffraction, 2002) using outlier rejection, scan speed scaling, as well as standard Lorentz and polarization correction factors. 79 594 reflections were merged to give 7818 unique data with an average redundancy of 10.2 and a mean $F^2/\sigma(F^2)$ of 12.58. The internal R index for the data set after reduction was 0.041 and the resolution of the data was up to 0.64 Å with a respectable mean $F^2/\sigma(F^2)$ of 1.90 for the ultra-high-angle data (0.66–0.64 Å resolution).

The structure was solved in the monoclinic space group $C2/c$ using direct methods in *WinGX*'s (Farrugia, 1999) implementation of *SHELXS*97 (Sheldrick, 1997). All non-H atoms were located in the E-map and refined anisotropically with *SHELXL*97 (Sheldrick, 1997). The data set was of sufficiently high quality that all the H atoms were located in the final difference-Fourier synthesis cycle. Since initial inspection of the difference map indicated the likely existence of two (aryl)C—H···O(nitro) hydrogen bonds, all H-atom coordinates were refined isotropically without constraints. The final isotropic temperature factors for the H atoms were acceptable, ranging from 0.027 (5) to 0.039 (6) Å^2. Since the refined (aryl)C—H distances measured 0.95 (2)–0.98 (2) Å, *i.e.* were in good agreement with the standard distance of 0.95 Å employed in constrained H-atom refinements, the model was deemed sufficient and no further refinement steps were therefore undertaken. The experimental details are given in full in Table 1.[1]

2.4. Molecular simulations

Molecular mechanics calculations were performed with *HyperChem*6.03 (Hypercube, 2000) using our previously published (Munro *et al.*, 2003[2]) force-field parameters (an augmented *MM*+ parameter set with electrostatics based on a bond-dipole model). Compound (4) has six degrees of torsional freedom involving the two sulfonic ester groups. Conformational searches were therefore conducted using a random torsion-angle-varying algorithm based on that published by Chang and co-workers (Chang *et al.*, 1989) in which the six torsion angles were varied randomly in 45° increments to generate a maximum of 10^4 random starting structures for geometry optimization (refinement cut-off: 0.033 kJ mol^{-1} between consecutive least-squares cycles). Starting conformations that matched already located conformations to within 3° for all six torsion angles and to within 0.356 kJ mol^{-1} in energy were discarded. A total of 1800 conformers were geometry optimized, locating 258 potentially unique low-energy conformations lying within 0–25 kJ mol^{-1} of the lowest-energy conformation. Inspection of these conformations revealed that there were of the order of 10–12 unique stable conformations (disregarding symmetry-related structures).

Semi-empirical quantum mechanics calculations (*AM*1 method, RHF wavefunction, singlet ground state; Dewar *et al.*, 1985) were performed with *Spartan*'04 (Wavefunction, 2004) using the X-ray or *MM*-calculated coordinates of (4) as input. [We have not employed higher-level electronic structure theory calculations on (4) in this study owing to the large size of its extended or 'supramolecular' structures.] Full geometry optimizations (refinement cut-off = 8.37 kJ mol^{-1}) of up to three hydrogen-bonded asymmetric units were used to investigate the hydrogen-bonding between molecules of (4) in the crystal lattice. Frequency calculations were performed on each optimized structure; no imaginary vibrational modes were found, suggesting that each structure was a true minimum on the potential energy surface for the system.

3. Results and discussion

3.1. Molecular and crystal structure of (4)

The X-ray crystal structure of (4) (Fig. 1) has crystallographically required C_2 symmetry; the twofold axis runs through the plane of the benzene ring (catechol moiety), bisecting the bonds C7—C7^{i} and C9—C9^{i} [symmetry code: (i) $-x, y, \frac{1}{2} - z$]. The two sulfonic ester groups are therefore located on opposite sides of the catechol-derived central aryl ring. The *trans* arrangement for the two nosylate groups evidently reflects their intrinsic steric bulk and the fact that such a conformation is likely to have a lower conformational energy than a *cis* arrangement. This argument is confirmed by our *MM* simulations (*see below*), which indicate that the lowest energy conformers of (4) have the two nosylate groups *trans*. The bond distances and angles involving the non-H atoms of (4) are not unusual in any way and have not been tabulated for conciseness. As far as the synthesis of (4) is concerned, this is the first structurally characterized example of the conversion of an aromatic 1,2-diol to a bis(sulfonic ester) – a feat that we were initially sceptical of based upon the

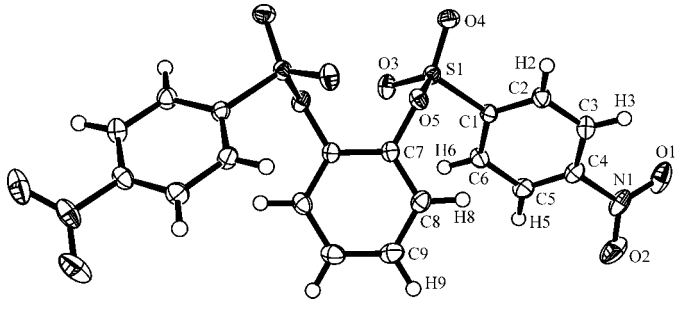

Figure 1
Labelled thermal ellipsoid diagram of the molecular structure of (4) (*ORTEP*3; Farrugia, 1997). Displacement ellipsoids are drawn at the 60% probability level; H atoms are drawn as spheres with equal, but arbitrary, radii.

[1] Supplementary data for this paper are available from the IUCr electronic archives (Reference: DE5007). Services for accessing these data are described at the back of the journal.

[2] The following force-field parameters were added to our augmented *MM*+ parameter set to facilitate the present simulations on aryl sulfonic esters. Torsion angle rotation (dihedral angle, V_1/kJ mol^{-1}, V_2/kJ mol^{-1}, V_3/kJ mol^{-1}): Csp^2—Ssp^3—Osp^3—Csp^2, 8.792, 1.130, 0.389; Csp^2—Osp^3—Ssp^3—Osp^2, 0.000, 0.000, 2.093; and Csp^2—Csp^2—Osp^3—S(sp^3), 0.000, 0.000, 0.000.

possible steric encumbrance that normally plagues reactions at adjacent functional groups on aryl rings (Munro *et al.*, 2004).

The plane of the nitro group of (4) is significantly tilted with respect to the phenyl group to which it is appended (C1–C6). The dihedral angle, which measures 33.6 (2)°, would normally be expected to be closer to 0° for a group containing an sp^2-hybridized nitrogen that is fully conjugated with the aryl ring. From Fig. 1 and a detailed analysis of the atomic temperature factors for the structure of (4) with the program *THMA*11 (Schomaker & Trueblood, 1968; Dunitz & White, 1973), it is evident that the anisotropic thermal displacement parameters for the atoms comprising the nitro group are quite normal and in no way suggestive of rotational disorder about the N1—C4 bond. The principal axes of the thermal ellipsoids of O1 and O2 are, in fact, consistent with an in-plane scissor (bending) vibrational mode for the nitro group. What causes a sizeable out-of-plane displacement for the nitro group of (4) if thermal motion in a direction approximately perpendicular to the C1–C6 plane is not culpable? Before answering this question, it is noteworthy that the dihedral angle between the nosylate aryl group (C1–C6) and the catechol-derived aryl group (C7–C9) is a substantial 37.8 (1)° and that there are no short intramolecular contacts between these two rings that might be indicative of intramolecular π–π interactions in this system, as previously observed for (3) (Munro *et al.*, 2003).

We have used *PARST* (Nardelli, 1983) to analyse the intermolecular interactions in (4) and to specifically answer the question of why a sizeable out-of-plane tilt exists for the nitro groups of this system. Somewhat unexpectedly, (4) has an extended solid state or intermolecular structure that is characterized by a lock-and-key type molecular self-recognition motif, namely near-symmetrical pairs of (aryl)C—H···O(nitro) hydrogen bonds (Fig. 2). The nitro-group O atoms on one molecule act as the hydrogen-bond acceptors for a pair of adjacent aromatic C—H groups on the neighbouring molecule. The interaction distances are 2.56 (3) (H8···O2^{v}), 2.38 (2) (H9···O1^{v}), 3.357 (3) (C8···O2^{v}) and 3.291 (3) Å (C9···O1^{v}); the hydrogen-bond angles measure 139 (2) (C8—H8···O2^{v}) and 154 (2)° (C9—H9···O1^{v}) [symmetry code: (v) $-x+\frac{1}{2}, -y+\frac{1}{2}+2, -z$]. This pair of hydrogen-bonding interactions also leads to what appears to be a slight lengthening of the C—H bonds involved. Specifically, the distances C8—H8 and C9—H9 both measure 0.98 (2) Å, some 0.03 Å longer than the distances for the non-interacting C—H bonds C2—H2, C5—H5 and C6—H6, which are all 0.95 (2) Å. Although it might be argued that the experimental difference is statistically insignificant (a neutron diffraction experiment would be required to actually prove or dispute this), our *AM*1 simulations of this system (*see below*) unequivocally show that the C—H bond order is reduced for these two C—H groups as a consequence of hydrogen bonding and thus clearly support this interpretation of the X-ray data.

Further evidence of the geometrical consequences of the two (aryl)C—H···O(nitro) hydrogen bonds is the fact that the nitro-group O1 and O2 atoms of one molecule are constrained to lie nearly in the plane of the catechol-derived aryl ring (C7–C9) of the neighbouring molecule. This specifically requires that the nitro group tilts out of the plane of the aryl ring to which it is attached (C1–C6) in an effort to optimally hydrogen bond with the pair of aromatic C—H donor groups of the neighbouring molecule. As seen in Fig. 2, this unusual hydrogen-bond donor/acceptor interaction (complementarity) coupled with the conformational flexibility of (4) about the C1—S1—O5—C7 torsion angle leads to the formation of an extended structure with a zigzag arrangement for the hydrogen-bond pairs along the hydrogen-bonded polymer backbone. The axis of the one-dimensional hydrogen-bonded polymer chain runs parallel to the [101] face diagonal of the monoclinic unit cell. Interestingly, nitro-group rotation in response to hydrogen-bond formation has also been observed for dimethyl-4-nitropyridine *N*-oxide (Hanuza *et al.*, 1998).

Moreover, each one-dimensional hydrogen-bonded polymer chain in the crystal lattice interacts with neighbouring polymer chains on either side of itself by C—H···O(SO_2) hydrogen bonds that are characterized by the distances 2.46 (2) (H6···O4^{iii}) and 3.272 (3) Å (C6···O4^{iii}), with an interaction angle of 143 (2)° (C6—H6···O4^{iii}) [symmetry code: (iii) $-x+\frac{1}{2}, y+\frac{1}{2}, -z+\frac{1}{2}$]. This reflects the geometry of the polymer chain which positions two of the three sulfonic ester O atoms laterally along the outside edges of the extended or 'supramolecular' chain. Location of the hydrogen-bond acceptors along the outer extremities of the 'supramolecular' chain means that they are ideally positioned to interact with the aromatic C—H donors of the nosyl-group aryl rings belonging to the neighbouring polymer chains, particularly since these C—H groups are not involved in the primary hydrogen-bonding sequences with the nitro groups that lead to the polymeric architecture of (4). Although C—

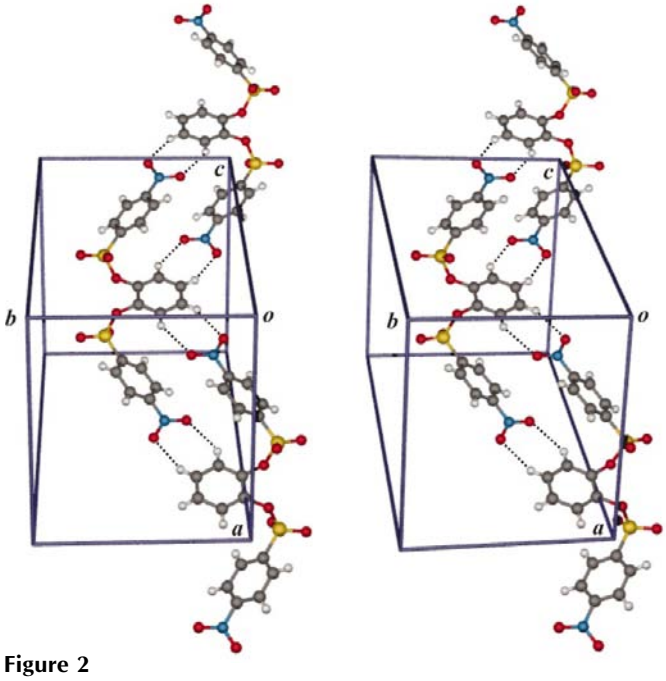

Figure 2
Stereoview of part of the unit-cell contents of (4). The remarkable role played by the nitro groups in the formation of a one-dimensional polymer by unusual pairs of (aryl)C—H···O(nitro) hydrogen bonds (broken lines) is clearly evident.

H···O hydrogen bonding is known and our interaction distances compare favourably with those in the literature (Bowes *et al.*, 2003), (4) presents an interesting case because this is the only kind of intermolecular interaction with a substantial stabilization energy that is in fact possible for this system. In short, with (4) we have a near-perfect opportunity to investigate the nature of these 'soft' hydrogen bonds in more detail. One last comment on the issue of intermolecular (lattice) interactions is in order for (4). There is a short O1···O3^{vi} contact [2.834 (4) Å, symmetry code: (vi) $x, 2-y, \frac{1}{2}+z$], which involves a nitro-group O atom of one molecule and a sulfonic ester-group O atom of a neighbouring molecule. Given the negative partial atomic charges for the O atoms of (4) (§3.3), this is an electrostatically unfavourable interaction.

3.2. Molecular mechanics simulations

As noted in §1, we have recently developed a new set of force-field parameters (*MM*+) for *MM* simulations of sulfonic esters (Munro *et al.*, 2003). An obvious question is whether the unique hydrogen bonding observed in the crystal structure of (4) locks in an unstable *molecular* conformation for the compound? If so, how unstable is this conformation relative to the minimum energy conformation of (4) in the absence of the crystal lattice (*i.e.* in the gas phase)? To answer these questions using theoretical methods, we have carried out a random search of the full conformational space available to (4) in the gas phase using *MM* methods. Use of a random search algorithm proved to be essential in this case since there are six degrees of torsional freedom for the molecule if we disregard the orientations of the nitro groups (which should remain coplanar with the aryl groups to which they are appended in the absence of hydrogen bonding). The search algorithm (Chang *et al.*, 1989) located of the order of 10–12 unique low-energy conformations of (4) lying within 25 kJ mol^{-1} of the lowest energy conformer.

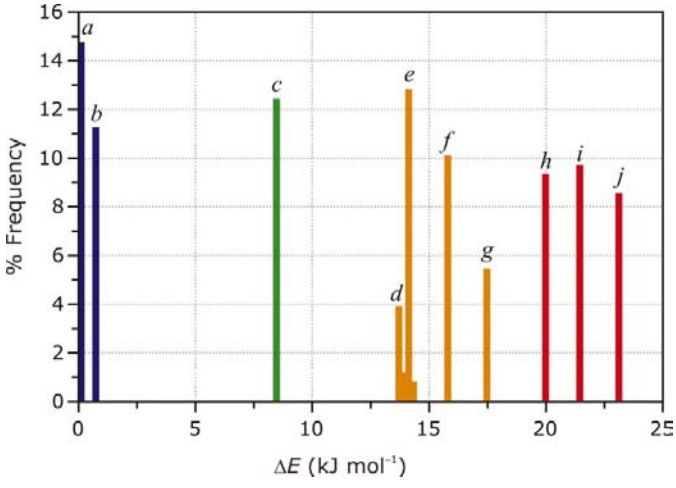

Figure 3
Distribution of 258 potentially unique low-energy conformations of (4) based on their relative steric energy values. The histogram shows the energies grouped in bins of 0.21 kJ mol^{-1} and clearly identifies that there are between 10 and 12 unique low energy conformations for (4).

Fig. 3 shows a frequency distribution of the lowest-energy conformers based on their steric energy values relative to the global minimum (note that conformations which are structurally unique but isoenergetic would not be differentiated by this plot). It is immediately apparent from the graph that the multi-dimensional conformational energy surface for (4) is characterized by numerous accessible minima. Moreover, the relative (or %) frequencies for each unique minimum taper off only gradually over the energy range plotted, consistent with the idea that the system is quite flexible. The lowest energy group of structures comprises two main conformer types [(4*a*) and (4*b*)] that fall in the narrow energy range of 0–1.05 kJ mol^{-1}. Since kT = 2.50 kJ mol^{-1} at 300 K, these would be abundantly populated in a gas-phase sample of the system at ambient temperatures. (It is noteworthy that a different conformer distribution may well be favoured in the presence of a solvent, but that such simulations are beyond the scope of the present investigation.)

There are three additional conformational clusters evident from Fig. 3 (based upon their relative steric energies). Conformer (4*c*) resides within a particularly tight energy band of 8.37–8.58 kJ mol^{-1} and stands alone in the distribution because of its separation from the next cluster of medium-energy conformers [(4*d*)–(4*g*)] by *ca* 5.23 kJ mol^{-1}. The four medium-energy conformers [(4*d*)–(4*g*)] that span the energy range 13.61–17.79 kJ mol^{-1} are followed by three higher-energy conformers that lie above 19.89 kJ mol^{-1} [(4*h*)–(4*j*)] in energy and are separated by roughly 2.09 kJ mol^{-1} increments within the cluster. Selected conformations taken from this

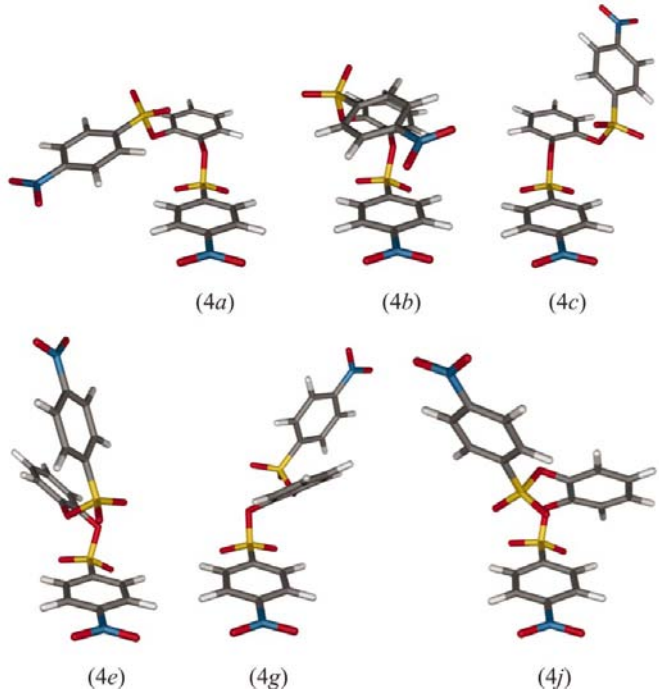

Figure 4
Selected low-energy conformations of (4) taken from the distribution of conformations shown in Fig. 3. (For consistency, only the first conformer located within a group was selected – the groupings are based on energy and do not distinguish symmetry-related conformers.)

Table 2
Steric energies and torsion-angle coordinates for geometry-optimized conformations (4*a*)–(4*j*) (calculated with a modified *MM*+ force field).

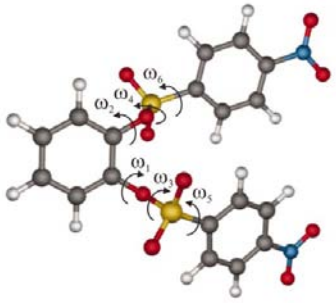

	ΔE	ω_1	ω_2	ω_3	ω_4	ω_5	ω_6
(4*a*)	0.00	−92.9	−92.9	−170.8	−170.9	95.8	95.9
(4*b*)	0.84	−88.7	−90.3	−174.8	−84.3	−79.9	−88.4
(4*c*)	8.46	94.1	98.8	172.0	−55.1	−88.2	95.0
(4*d*)	13.82	89.3	89.2	76.4	75.8	88.3	−95.1
(4*e*)	14.07	−97.2	−97.6	−99.4	58.3	105.5	−95.1
(4*f*)	15.74	85.3	−54.5	170.5	−145.4	98.8	111.3
(4*g*)	17.50	−95.2	−95.2	62.3	62.4	87.7	−96.0
(4*h*)	20.10	−52.6	93.6	−155.2	−43.4	108.3	−88.7
(4*i*)	21.44	69.0	−60.0	166.2	−52.7	91.8	−101.9
(4*j*)	23.07	62.2	−88.3	50.6	137.2	−82.9	−93.5

ΔE: Relative steric energy in kJ mol^{-1}; ω values: torsion angles (°).

distribution are shown in Fig. 4. The conformational energy data and torsion angle coordinates for the first located conformation within each conformer group (4*a*)–(4*j*) are summarized in Table 2.

The lowest energy conformations (4*a*) and (4*b*) have their nitrobenzene rings relatively closely spaced with the plane of each nitrobenzene ring approaching a roughly parallel configuration that is suggestive of stabilization by intramolecular $\pi\cdots\pi$ interactions (Hunter *et al.*, 2001), as previously observed for nosylate (3) (Munro *et al.*, 2003). The remaining conformations adopt a more open (splayed apart) configuration for the nosylate groups and exhibit higher steric energies. The most interesting of these is a C_2 symmetry conformation that fairly closely matches the crystal structure of (4), namely conformer (4*g*). The existence of a gas-phase conformation that is similar to the X-ray conformation is to some extent expected, unless one has a transition state trapped in the crystal lattice, in which case none of the low-energy gas-phase conformers would match the crystal structure. However, the most important fact remains that the X-ray conformation of (4) in the absence of the crystal lattice environment is *not* the lowest-energy conformation for this system. The X-ray conformation of (4) in fact lies ∼26.54 kJ mol^{-1} higher in energy than the global minimum (*cf.* Fig. 5*b*). This clearly demonstrates that the unique (aryl)C—H···O(nitro) hydrogen bonding observed in the crystal structure of (4) favours the crystallization of a relatively unstable conformation of the molecule, presumably to optimize the formation of the hydrogen-bonded (polymeric) chains illustrated in Fig. 2. It therefore seems likely that in the case of (4), a more favourable lattice energy is achieved with a C_2 symmetry conformer at the expense of conformational stability.

As shown in Fig. 5 the crystal lattice is fundamental in determining the observed conformation of (4) in the solid state. The r.m.s. (root-mean square) fit of the gas-phase conformation (4*g*) to the X-ray conformation is poor (r.m.s.d. = 1.79 Å) and shows that the orientations of the nosylate groups in the calculated structure differ significantly from those of the experimental structure. Moreover, the calculated structure predicts that the nitro groups are coplanar with the aryl rings to which they are appended as a result of conjugation. In the experimental structure, the dihedral angle between the nitro groups and the appended aryl ring measures 33.6 (2)° – a situation that reflects the conformational adjustments needed to optimize the intermolecular hydrogen bonds involving the nitro groups in the solid state (*see above*). The gas-phase structure (4*g*) obviously does not include these highly significant interactions and thus adopts a conformation that is lower in energy by 9.04 kJ mol^{-1} with ω_3 values of 62.4° [as opposed to 77.9 (1)° in the X-ray crystal structure]. Fig. 5(*b*) clearly shows that when all neighbouring molecules in the crystal lattice are included in the simulation, the calculated conformation of (4) closely matches that observed in the X-ray crystal structure (r.m.s.d. = 0.211 Å). Not only do the nosylate groups correctly match the positions of those in the experimental structure, but the nitro-group orientations of 37.8° are seen to be in good agreement with those of the X-ray structure.

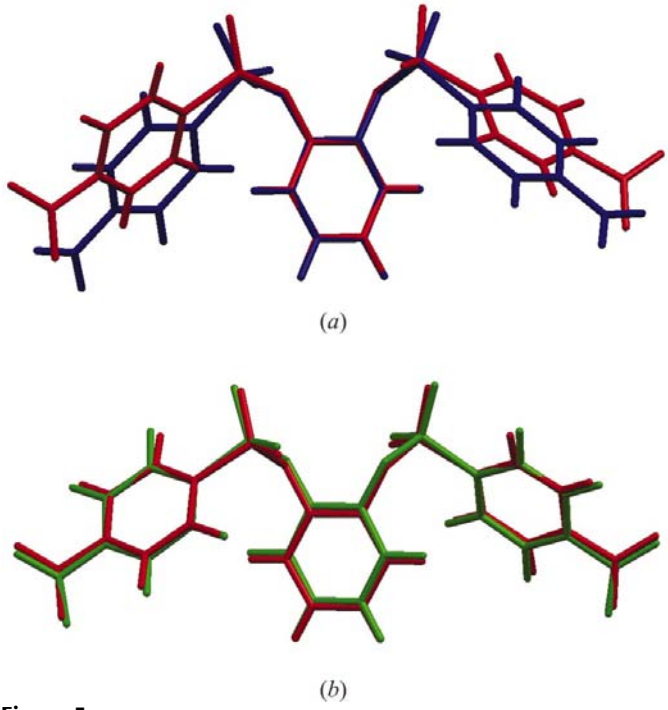

Figure 5
Root-mean-square (r.m.s.) fits of the X-ray crystal structure of (4) (red) to (*a*) the gas-phase geometry-optimized conformer (4*g*) (ΔE = 17.50 kJ mol^{-1}, blue structure) and (*b*) the conformation of (4) calculated in the presence of all neighbouring molecules in the crystal lattice (ΔE = 26.54 kJ mol^{-1}, green structure).

The MM2 (Allinger, 1977) and *MM*+ force fields model hydrogen bonding with a dipole–dipole interaction potential. As evidenced by the present simulations, this model succeeds reasonably well even for relatively 'soft' (aryl)C—H···O(nitro) hydrogen bonds, provided that the simulation includes the neighbouring molecules in the crystal lattice. More specifically, Fig. 5(*b*) illustrates that when all of the possible intermolecular interactions (van der Waals forces, dipole–dipole interactions and hydrogen-bonds) are included in the calculation, an accurate conformation prediction is possible. The simulations thus highlight the critical role played by the crystal lattice (and ultimately the lattice enthalpy, which drives the formation of a particular lattice structure) in determining the observed solid-state structure of (4).

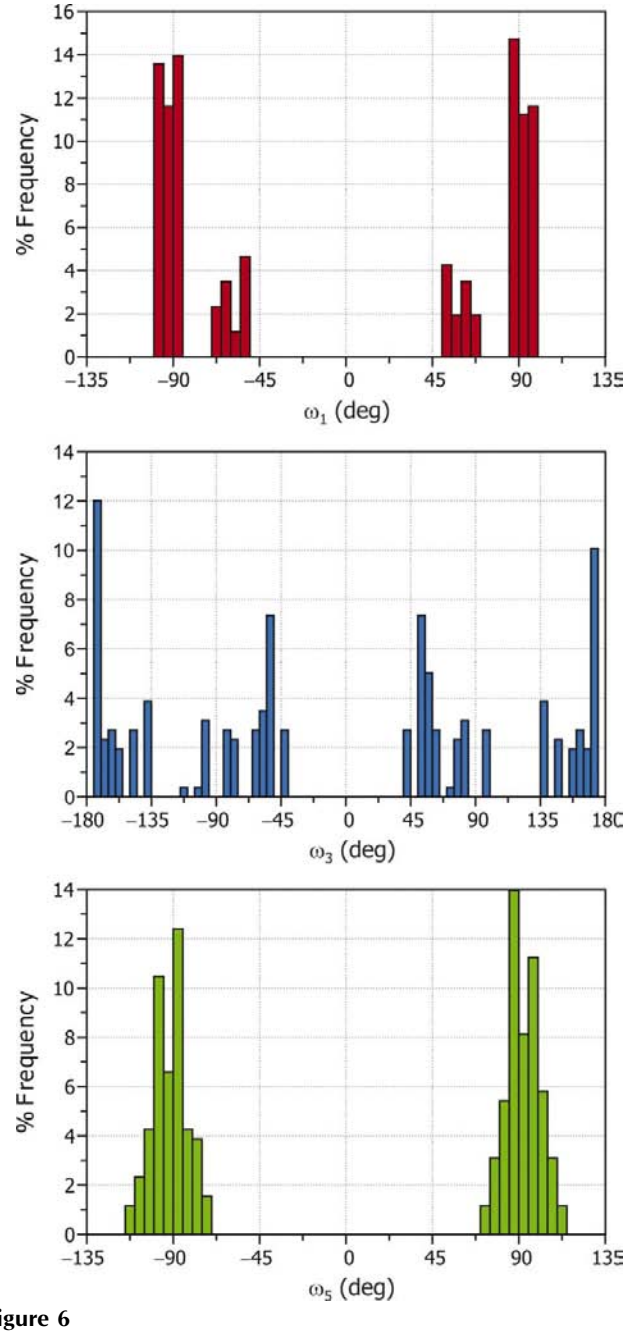

Figure 6
Symmetry-unique torsion-angle distributions for the 258 geometry-optimized potentially unique low-energy conformations of (4) found during an *in vacuo* random search of the accessible conformational space for the molecule. The torsion angles are defined in Table 2.

Inspection of the torsion angles listed in Table 2 for the calculated low-energy conformations of (4) suggests that ω_3 and ω_4 are the most variable. In Fig. 6 we have plotted the distribution of one set of torsion angles (ω_1–ω_3) of the pair which govern the orientations of the nosylate groups for the 258 potentially unique low-energy conformations of (4) located in the conformational search. The first torsion angle ω_1 adopts only two possible mean orientations, namely ∼60 and ∼90°. The same distribution holds for the chemically identical torsion angle ω_2. As might be anticipated from increased intramolecular steric strain [benzene ring···O(SO_2) interactions], conformations having ω_1 close to 60° are higher in energy than those having ω_1 ∼90°. The fifth torsion angle, ω_5, which governs the orientation of the nitrobenzene ring relative to the (ArO)SO_2 group is the least variable and gives a symmetrical normal distribution with a mean of ∼90°. The same distribution holds for the chemically identical torsion angle ω_6. At first glance, it is quite surprising that this torsion angle should be rigorously near 90°. However, orientations of 0 or 180° would bring the *o*-H atoms of the nitrobenzene ring into the same plane as the S—O—Ar group and would clearly lead to rather severe H···O non-bonded repulsion. Finally, the third torsion angle (and by chemical equivalence the fourth) is the most variable. This involves rotation about the Ar—O—$S(O_2)$—Ar bond within the molecule. As seen in Fig. 6, there is a fair spread in the possible orientations that ω_3 may adopt. However, angles of ∼60° and ∼180° are clearly more frequently found, while angles of ∼0–40° and ∼120° are absent from the observed range of values for this variable. When ω_3 = 0°, the nitrobenzene ring would be forced to lie directly over the central aryl ring. As the O—S—Ar bond angle is 104.9° for the sp^3 hybridized S atom, the nitrobenzene ring atoms would penetrate the region of space occupied by the central aryl ring C and H atoms and this would lead to a colossal increase in the strain energy (non-bonded repulsion) for the system. Such conformations are thus rigorously avoided. Collectively, the histograms shown in Fig. 6 confirm that the conformational flexibility of (4) derives mainly from rotations about ω_3 and ω_4.

3.3. MO theory calculations

We have recently studied several compounds which display interesting supramolecular structures that are stabilized by complementary N—H···N hydrogen bonding both in the solid state (Munro & Camp, 2003) and in solution (Munro *et al.*, 2004). As supramolecular hydrogen-bonded systems are often large in size (dimers, trimers and polymers), the most feasible quantum mechanical technique for studying their electronic structures is a semi-empirical method such as *AM*1 (Dewar *et al.*, 1985), in which only the valence electrons of the atoms are included in the simulation to expedite the calculations. Despite the approximations involved in the method, there is good evidence to indicate that semi-empirical MO simulations

perform well in modelling intermolecular hydrogen bonding (Bodige *et al.*, 1998; Testa, 1999; Santhosh & Mishra, 1998), including weak C—H···O interactions (Hajnal *et al.*, 1999; Thaimattam *et al.*, 2001).

Traditionally, two approaches are used to model hydrogen bonds, namely dipole–dipole interactions and electrostatic interactions (Jensen, 1999). The former approach is restricted to simulations with *MM* force fields, while the latter method applies to either *MM* simulations (in which partial charges are calculated prior to their inclusion in the simulation) or quantum mechanical methods. In the present case we have studied the monomer and hydrogen-bonded dimer forms of (4) using *in vacuo* *AM*1 simulations in order to shed further light on the electronic structure of this system, particularly since the *MM* simulations of §3.2 strongly suggest that the inclusion of hydrogen bonding between individual molecules of (4) is critical to an accurate simulation of the structure of this compound. The results of our *AM*1 calculations are consistent with the main conclusions drawn from the *MM* simulations. Specifically, as shown in Fig. 7(*a*), the structure of the monomer calculated in the gas phase deviates significantly from the X-ray crystal structure of (4) (r.m.s.d. = 1.03 Å), although it is a somewhat better match than the conformation calculated with the *MM*+ force field. The nitro groups are coplanar with the aryl ring to which they are appended and the main deviation is a rotation about the flexible torsion angles ω_3 and ω_4. As noted in §3.2, this reflects the fact that the crystal lattice environment plays a critical role in fixing the orientations of the nitrobenzene groups as a result of intermolecular (aryl)C—H···O(nitro) hydrogen bonds. Although we cannot carry out an *AM*1 simulation of the full crystal lattice at present, the calculated structure of the hydrogen-bonded dimer shown in Fig. 7(*b*) is clearly a better match of the crystal structure (r.m.s.d. = 0.430 Å). Inclusion of two of the key intermolecular interactions in this system therefore dramatically improves the agreement between the experimental and theoretical structures.

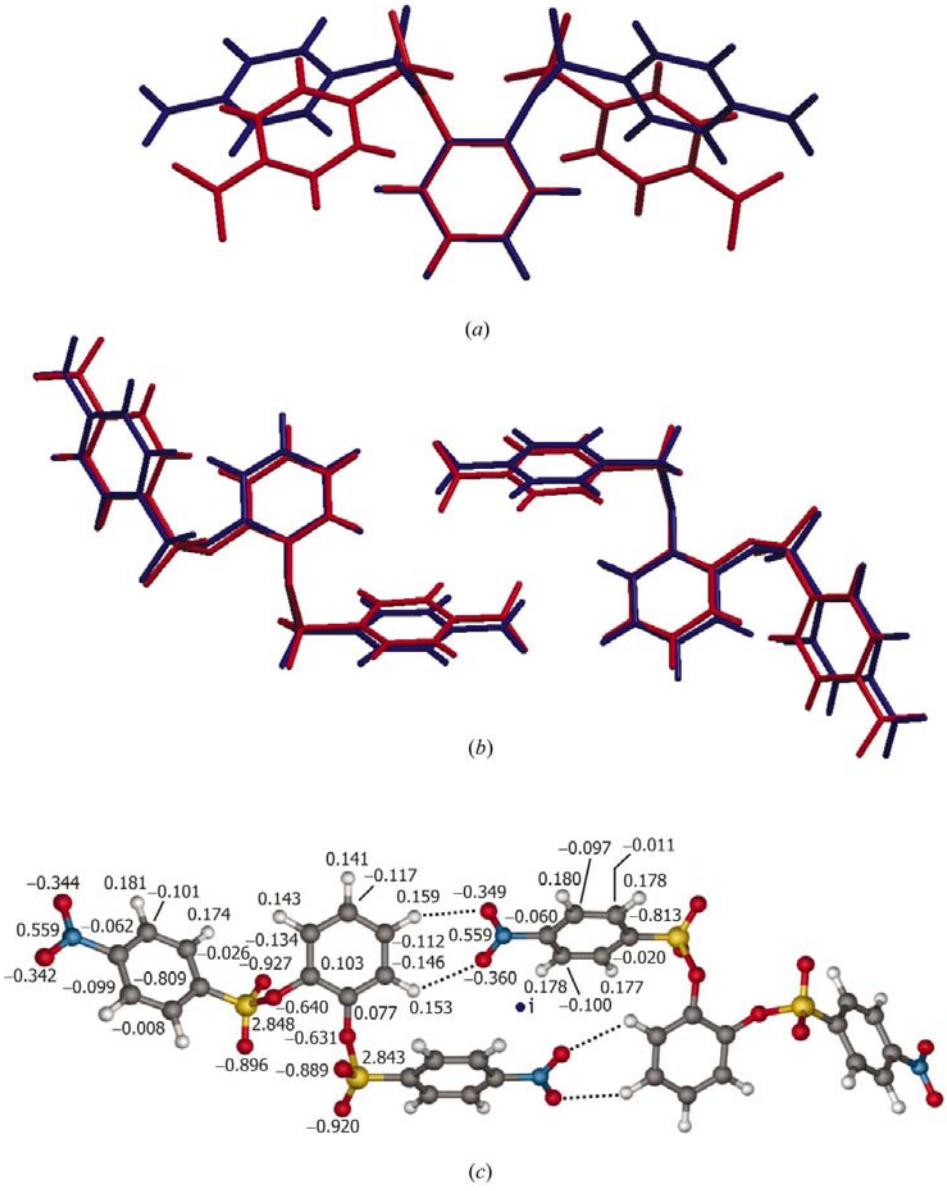

Figure 7
(*a*) Root-mean-square fit of the X-ray (red) and *AM*1-calculated (blue) monomer structures of (4). (*b*) Root-mean-square (r.m.s.) fit of the X-ray (red) and *AM*1-calculated (blue) dimer structures of (4). (*c*) *AM*1-calculated geometry of the hydrogen-bonded dimer of (4). The dimer has C_i symmetry with the centre of inversion indicated. Natural atomic charges for symmetry unique atoms are shown.

The *in vacuo* enthalpy of association for a dimer, $\Delta H_{\rm ass}$, may be calculated using *AM*1 by subtracting the heat of formation of the dimer at infinite separation (*i.e.* roughly > 20 Å, and with the structural units comprising the dimer having unchanged conformations), ΔH^{∞}, from the heat of formation of the associated complex, $\Delta H_{\rm dimer}$, and correcting for the basis-set superposition error (BSSE), as given in (1)

$$\Delta H_{\rm ass} = \Delta H_{\rm dimer} - \Delta H^{\infty} - {\rm BSSE}. \quad (1)$$

The BSSE for the structure shown in Fig. 7(*c*) was calculated to be −0.119 kJ mol^{-1}, *i.e.* basis-set superposition leads to a small overestimation of the stability of the dimer, as noted elsewhere (Jensen, 1999). Since $\Delta H_{\rm dimer}$ and ΔH^{∞} were −917.49 and −901.17 kJ mol^{-1}, respectively, $\Delta H_{\rm ass}$ = −15.63 kJ mol^{-1} for the dimer structure of (4). Given that the net

Table 3
Selected *AM*1 calculated vibrational frequencies for (4).

	Frequency (cm^{-1})		
Vibrational mode	Monomer	Dimer	
ν_s (NO_2)	1785.7	1795.7†	1786.3‡
ν_a (NO_2)	2068.5	2056.3†	2067.8‡
ν_a (CH)	3181.4§	3161.6§	

† Hydrogen-bonded nitro group. ‡ Terminal nitro group. § Antisymmetric C—H stretching mode for the *o*- and *m*-CH groups of the central aryl ring.

stabilization energy per hydrogen bond is usually between −3.00 and −5.00 kJ mol^{-1} (Clote & Backofen, 2000), the average stabilization energy per hydrogen bond calculated for the dimer structure of (4) (−3.91 kJ mol^{-1}) is in fact surprisingly good for a computational method that treats only the valence electrons and does not directly take into account electron correlation effects. Moreover, our calculations showed that the loss of resonance stabilization energy associated with tipping the hydrogen-bonded nitro groups out of the plane of their parent benzene rings was only +1.29 kJ mol^{-1} (for two out-of-plane rotations of 16°). The stability gained on hydrogen-bond formation therefore readily exceeds this energy penalty and confirms that the main driving force behind the rotation of the nitro groups in (4) is (aryl)C—H···O(nitro) hydrogen-bond formation. Interestingly, despite the fact that the hydrogen-bonded nitro groups in the dimer are calculated to have orientations of only 16.2° (*i.e.* about half the value observed in the experimental structure), the calculated hydrogen-bond distances are in good agreement with those of the X-ray structure. More specifically, the H9···O1 and H8···O2 distances (§3.1) measure 2.44 and 2.63 Å in the calculated structure, respectively, and thus compare favourably with the experimental distances of 2.38 (2) and 2.56 (3) Å. Fig. 7(*c*) shows the natural atomic charges for the calculated dimer structure of (4). The (aryl)C—H···O(nitro) hydrogen-bonding interactions are clearly favoured on electrostatic grounds. The two nitro-group O atoms carry partial negative charges of −0.349 and −0.360 *e* and thus complement the positive partial charges carried by the *o*- (0.153 *e*) and *m*-hydrogen (0.159 *e*) atoms of the central aryl ring of the neighbouring molecule.

Finally, since we carried out frequency calculations on the monomer and dimer structures of (4) at the *AM*1 level of theory to confirm that all calculated structures were true minima, the effect of hydrogen bonding on the nitro group vibrational modes in this system may be assessed. While it is well known that *AM*1 cannot accurately calculate the absolute frequencies of the vibrations for a molecule, the method is suitable for estimating the relative frequency shifts of key vibrational modes for structurally related molecules.

Table 3 lists selected vibrational frequencies for the *AM*1-calculated monomer and dimer structures of (4). The symmetric stretching vibration of the nitro group shifts by 10.0 cm^{-1} to a higher frequency, while the antisymmetric stretching mode decreases by 12.2 cm^{-1} upon hydrogen-bond formation. The frequency difference between the symmetric and antisymmetric modes therefore decreases from 282.8 to 260.6 cm^{-1} with the formation of a pair of (aryl)C—H···O(nitro) hydrogen bonds. Despite the fact that the absolute frequencies are calculated to be too high by roughly 500 cm^{-1} (mainly because of the approximate level of theory), it is interesting to note that the calculated relative separation of the symmetric and antisymmetric stretching vibrations more closely matches the experimental value of 173 cm^{-1}. The C—H groups of the central aryl ring are also substantially affected by the hydrogen-bonding interactions. In particular, the frequency of the antisymmetric stretching mode decreases by 19.8 cm^{-1} upon hydrogen-bond formation. Collectively, the calculations suggest that the intermolecular hydrogen-bonding interactions in (4) perturb the formal N—O and C—H bonds involved in the interaction by very slightly decreasing their bond orders. Not only is this result consistent with the slight lengthening of the two C—H bonds observed in the crystal structure of (4), but similar perturbations of the vibrational frequencies of hydrogen-bonded nitro groups have been observed experimentally by IR and Raman spectroscopy (Quaroni & Smith, 1999; Hanuza *et al.*, 1998; Dubis *et al.*, 1998) and in quantum theory simulations of such systems (Carper *et al.*, 1993).

4. Summary and conclusions

Compound (4), the novel bis(nosylate) derivative of catechol, has been synthesized and characterized by several methods including low-temperature single-crystal X-ray diffraction. The compound crystallizes in the monoclinic space group *C*2/*c*; the asymmetric unit lies on a twofold axis of rotation and the molecular point-group symmetry is C_2. The C_2 symmetry conformation is crucial for the formation of a chain-like hydrogen-bonded structure, which is mediated by a near-equivalent pair of (aryl)C—H···O(nitro) hydrogen bonds between each nitro group and a neighbouring molecule's central aryl ring. Molecular mechanics simulations indicate that the X-ray conformation of (4) is not the most stable, lying ∼26.5 kJ mol^{-1} higher in energy than the C_1 symmetry *in vacuo* global minimum and ∼9.0 kJ mol^{-1} higher in energy than the analogous gas-phase conformer with C_2 symmetry. Since the most accurate calculation of the conformational architecture of (4) was achieved when all neighbouring molecules in the crystal lattice were included in the simulation, we conclude that the unique hydrogen bonding in conjunction with intermolecular non-bonded interactions in (4) play a highly significant role in determining the solid-state structure of this compound. This conclusion is supported by *AM*1 simulations which confirm that the (aryl)C—H···O(nitro) hydrogen bonds direct the conformation of the structure at the intermolecular or 'supramolecular' level and that the electrostatics of the interaction are complementary.

We gratefully acknowledge financial support from the University of KwaZulu-Natal and the National Research Foundation (NRF, Pretoria).

References

Allinger, N. L. (1977). *J. Am. Chem. Soc.* **99**, 8127–8134.
Bemm, U. & Ostmark, H. (1998). *Acta Cryst.* C**54**, 1997–1999.
Bodige, S. G., Zottola, M. A., Mckay, S. E. & Blackstock, S. C. (1998). *Mater. Res. Bull.* pp. 243–253.
Bowes, K. F., Ferguson, G., Lough, A. J. & Glidewell, C. (2003). *Acta Cryst.* B**59**, 100–117.
Braga, D., Grepioni, F., Biradha, K., Pedireddi, V. R. & Desiraju, G. R. (1995). *J. Am. Chem. Soc.* **117**, 3156–3166.
Carey, F. A. & Sundberg, R. J. (1990). *Advanced Organic Chemistry*, 3rd. ed., pp. 579–583. New York: Plenum Press.
Carper, W. R., Zandler, M. & Mains, G. J. (1993). *J. Phys. Chem.* **97**, 9091–9095.
Chang, G., Guida, W. C. & Still, W. C. (1989). *J. Am. Chem. Soc.* **111**, 4379–4386.
Chen, P. C. & Tzeng, S. C. (1999). *J. Mol. Struct. Theochem.* **467**, 243–257.
Clote, P. & Backofen, R. (2000). *Computational Molecular Biology: An Introduction*, pp. 3–17. New York: Wiley.
Coupar, P. I., Glidewell, C. & Ferguson, G. (1997). *Acta Cryst.* B**53**, 521–533.
Del Bene, J. E. & Kochenour, W. L. (1976). *J. Am. Chem. Soc.* **98**, 2041–2046.
Desiraju, G. R. & Steiner, T. (1999). *The Weak Hydrogen Bond in Structural Chemistry and Biology*. Oxford University Press.
Dewar, M. J. S., Zoebisch, E. G., Healy, E. F. & Stewart, J. P. P. (1985). *J. Am. Chem. Soc.* **107**, 3902–3909.
Dubis, A. T., Lotowski, Z., Siergiejczyk, L., Wilczewska, A. Z. & Morzycki, J. W. (1998). *J. Chem. Res. S*, **4**, 170–171.
Dunitz, J. D. & White, D. N. J. (1973). *Acta Cryst.* A**29**, 93–94.
Farrugia, L. J. (1997). *J. Appl. Cryst.* **30**, 565.
Farrugia, L. J. (1999). *J. Appl. Cryst.* **32**, 837–838.
Ferguson, G., Coupar, P. I. & Glidewell, C. (1997). *Acta Cryst.* B**53**, 513–520.
Hajnal, Z., Keseru, G. M. & Simon, K. (1999). *J. Mol. Struct. Theochem.* **463**, 169–174.
Hanuza, J., Maczka, M., Waskowska, A., Oganowski, W., Banoganowska, H., Lutz, E. T. G. & Vandermaas, J. H. (1998). *J. Mol. Struct.* **450**, 201–212.
Hunter, C. A., Lawson, K. R., Perkins, J. & Urch, C. J. (2001). *J. Chem. Soc. Perkin Trans. 2*, pp. 651–669.
Hypercube (2000). *HyperChem*, Version 6.03. Hypercube Inc., 1115 NW 4th Street, Gainsville, FL 32601–4256, USA.
Jensen, F. (1999). *Introduction to Computational Chemistry*. Chichester: John Wiley and Sons.
Langley, P. J., Hulliger, J., Thaimattam, R. & Desiraju, G. R. (1998). *New J. Chem.* **22**, 1307–1309.
Leiserowitz, L. (1976). *Acta Cryst.* B**32**, 775–802.
March, J. (1985). *Advanced Organic Chemistry*, 3rd ed. New York: John Wiley and Sons.
Mowbray, C. E., Skranc, W. & Wallis, J. D. (1999). *J. Chem. Crystallogr.* **29**, 335–341.
Munro, O. Q. & Camp, G. L. (2003). *Acta Cryst.* C**59**, o672–o675.
Munro, O. Q., McKenzie, J. M., Strydom, S. D. & Gravestock, D. (2003). *J. Org. Chem.* **68**, 2448–2459.
Munro, O. Q., Strydom, S. D. & Grimmer, C. (2004). *New J. Chem.* **28**, 34–42.
Nardelli, M. (1983). *Comput. Chem.* **7**, 95–97.
Oxford Diffraction (2002). *CrysAlis CCD* and *CrysAlis RED*. Versions 170. Oxford Diffraction Ltd, Abingdon, UK.
Quaroni, L. & Smith, W. E. (1999). *J. Raman Spectrosc.* **30**, 537–542.
Rablen, P. R., Lockman, J. W. & Jorgensen, W. L. (1998). *J. Phys. Chem. A*, **102**, 3782–3797.
Santhosh, C. & Mishra, P. C. (1998). *Int. J. Quantum Chem.* **68**, 351–355.
Schomaker, V. & Trueblood, K. N. (1968). *Acta Cryst.* B**24**, 63–76.
Sheldrick, G. M. (1997). *SHELXS*97 and *SHELXL*97. University of Göttingen, Germany.
Sørensen, H. O. & Larsen, S. (2003). *Acta Cryst.* B**59**, 132–140.
Szczesna, B. & Urbanczyk-Lipkowska, Z. (2002). *New J. Chem.* **26**, 243–249.
Testa, A. C. (1999). *Spectrosc. Lett.* **32**, 819–828.
Thaimattam, R., Xue, F., Sarma, J. A. R. P., Mak, T. C. W. & Desiraju, G. R. (2001). *J. Am. Chem. Soc.* **123**, 4432–4445.
Wavefunction (2004). *Spartan*'04. Wavefunction Inc., Irvine, CA.
Wolff, J. J., Gredel, F., Oeser, T., Irngartinger, H. & Pritzkow, H. (1999). *Chem. Eur. J.* **5**, 29–38.
Yan, H. & Zhu, X. (1999). *J. Appl. Polym. Sci.* **74**, 97–105.